

Improved sensitivity on the electromagnetic dipole moments of the top quark in $\gamma\gamma$, $\gamma\gamma^*$ and $\gamma^*\gamma^*$ collisions at the CLIC

A. A. Billur*

Department of Physics, Cumhuriyet University, 58140, Sivas, Turkey.

M. Köksal†

Department of Optical Engineering, Cumhuriyet University, 58140, Sivas, Turkey.

A. Gutiérrez-Rodríguez‡

Facultad de Física, Universidad Autónoma de Zacatecas

Apartado Postal C-580, 98060 Zacatecas, México.

Abstract

We realize a phenomenological study to examine the sensitivity on the magnetic moment and electric dipole moment of the top quark through the processes $\gamma\gamma \rightarrow t\bar{t}$, $e\gamma \rightarrow e\gamma^*\gamma \rightarrow e\bar{t}t$ and $e^-e^+ \rightarrow e^-\gamma^*\gamma^*e^+ \rightarrow e^-t\bar{t}e^+$ at the CLIC. We find that with a center-of-mass energy of the CLIC-1.4 TeV, integrated luminosity of $\mathcal{L} = 1500 fb^{-1}$ and CLIC-3 TeV, integrated luminosity of $\mathcal{L} = 2000 fb^{-1}$ with systematic uncertainties of $\delta_{sys} = 0, 5, 10 \%$ at the 95% C.L., it is possible the CLIC may put limits on the electromagnetic dipole moments of the top quark \hat{a}_V and \hat{a}_A with a sensitivity of $\mathcal{O}(10^{-3} - 10^{-2})$. Therefore, we show that the sensitivity with the CLIC data is much greater than that for the LHC data.

* abillur@cumhuriyet.edu.tr

† mkoksal@cumhuriyet.edu.tr

‡ alexgu@fisica.uaz.edu.mx

I. INTRODUCTION

The Standard Model (SM) has been tested in many important experiments and has been quite successful, particularly after the discovery of a particle consistent with the Higgs boson with a mass of about $125 \pm 0.4 \text{ GeV}$. On the other hand, some of the most fundamental questions still remain unanswered. For instance, the CP problem, neutrino oscillations and matter-antimatter asymmetry have not been adequately clarified by the SM. For this reason, it is often thought that the SM is embedded in a more fundamental theory with which its effects can be observed at higher energy scales.

The top quark is the most massive of all observed elementary particles in the SM. Because of the top quark's large mass, its couplings are expected to be more sensitive to new physics beyond the SM with respect to other particles. New physics can manifest itself in different forms. One possibility is that the new physics may lead to the appearance or a huge increase of new types of interactions like tH^+b or anomalous Flavor Changing Neutral Current tqg , $tq\gamma$ and tqZ ($q = u, c$) interactions. Another possibility is the modification of the SM couplings that involve $t\bar{t}g$, $t\bar{t}\gamma$, $t\bar{t}Z$ and tWb vertices.

CP violation was first discovered in a small fraction of the kaon decays. This phenomenology can be easily introduced by the Cabibbo-Kobayashi-Maskawa matrix (CKM) in the quark sector. CP violation in this sector is not enough to clarify the baryon asymmetry in the universe. This asymmetry is one of the basic problems in the SM that has not been resolved even in the heavy quarks decay processes. Therefore, the measurement of large amounts of CP violation in the top quark processes in colliders can demonstrate new physics. The existence of new physics can be analyzed by investigating the electromagnetic properties of the top quark that are determined with its dipole moments such as the Magnetic Dipole Moment (MDM) and Electric Dipole Moment (EDM) defined as a source of CP violation.

The projection in the SM for the MDM of the top quark is $a_t^{SM} = 0.02$ [1], and can be tested in the current and future colliders such as the Large Hadron Collider (LHC) and the Compact Linear Collider (CLIC). In contrast, the EDM of the top quark is strongly suppressed with a value of less than $10^{-30} e \text{ cm}$ [2–4], and is much too small to be observed. However, it is very attractive for probing new physics. If there is a new physics beyond the SM, the top quark may have a higher EDM value than $10^{-30} e \text{ cm}$. It is worth mentioning

that the sensitivity to the EDM has been studied in models with vector like multiplets which predicted the top quark EDM close to 1.75×10^{-3} [5].

The studies performed through the $t\bar{t}\gamma$ production for the LHC at $\sqrt{s} = 14\text{ TeV}$, $\mathcal{L} = 300\text{ fb}^{-1}$ and 3000 fb^{-1} reported the limits of ± 0.2 and ± 0.1 , respectively [6]. The limits $-2.0 \leq \hat{a}_V \leq 0.3$ and $-0.5 \leq \hat{a}_A \leq 1.5$ are obtained from the branching ratio and the CP asymmetry from radiative $b \rightarrow s\gamma$ transitions [7]. However, the authors of Ref. [8] obtained the bounds on $|\hat{a}_V| < 0.05$ (0.09) and $|\hat{a}_A| < 0.20$ (0.28) from measurements of the $\gamma^*p \rightarrow t\bar{t}$ cross section with 10% (18%) uncertainty at the Large Hadron electron Collider (LHeC), respectively. Bounds on the dipole moments of the top quark were recently reported in literature through the process $pp \rightarrow p\gamma^*\gamma^*p \rightarrow pt\bar{t}p$ for the energy and luminosity of the LHC of $\sqrt{s} = 14\text{ TeV}$, $\mathcal{L} = 3000\text{ fb}^{-1}$ and 68% C.L.: $-0.6389 \leq \hat{a}_V \leq 0.0233$ and $|\hat{a}_A| \leq 0.1158$ [9].

Moreover, in the case of the e^+e^- collider as the International Linear Collider (ILC), the sensitivity bounds at 1σ for the anomalous couplings of the top quark through top quark pair production $e^+e^- \rightarrow t\bar{t}$ at $\sqrt{s} = 500\text{ GeV}$, $\mathcal{L} = 200\text{ fb}^{-1}$, $\mathcal{L} = 300\text{ fb}^{-1}$ and $\mathcal{L} = 500\text{ fb}^{-1}$ are predicted to be of the order $\mathcal{O}(10^{-3})$, indicating that measurements at an electron positron collider lead to a significant improvement in comparison with the LHC. Thorough and detailed discussions on the dipole moments of the top quark in top quark pair production at the ILC are reported in the literature [10–21].

In Ref. [22], bounds are estimated on the electromagnetic dipole moments of the top quark through the processes $\gamma e^- \rightarrow \bar{t}b\nu_e$ and $e^+e^- \rightarrow e^-\gamma^*e^+ \rightarrow \bar{t}b\nu_e e^+$ with unpolarized and polarized electron beams at the CLIC. For the systematic uncertainties of $\delta_{sys} = 0\%$, 5%, b – tagging efficiency = 0.8, center-of-mass energy of $\sqrt{s} = 3\text{ TeV}$, integrated luminosity of $\mathcal{L} = 2000\text{ fb}^{-1}$ and 2σ (3σ), the bounds obtained on the electromagnetic dipole moments \hat{a}_V and \hat{a}_A of the top quark are of the order $\mathcal{O}(10^{-2} - 10^{-1})$ and are highly competitive with those reported in previous studies.

The advantage of the linear e^-e^+ colliders with respect to the hadron colliders is in the general cleanliness of the events where two elementary particles, electrons and positrons beams, collide at high energy, and the high resolutions of the detector made possible by the relatively low absolute rate of background events. In addition, these colliders will complement the physics program of the LHC, especially for precision physics. Therefore, precise measurements of the top quark properties, such as the mass, charge, spin and dipole mo-

ments will become possible. The CLIC is a proposed future e^-e^+ collider, designed to fulfill e^-e^+ collisions at center-of-mass energies of 0.35, 1.4 and 3 TeV planned to be constructed with a three main stage research region [23]. This enables the investigation of the $\gamma\gamma$ and $e\gamma$ interactions by converting the original e^- or e^+ beam into a photon beam through the Compton backscattering mechanism. The other well-known applications of the linear colliders are the processes $e\gamma^*$, $\gamma\gamma^*$ $\gamma^*\gamma^*$ where the emitted quasireal photon γ^* is scattered with small angles from the beam pipe of e^- or e^+ [24–29]. Since these photons have a low virtuality, they are almost on the mass shell. These processes can be described by the Weizsacker-Williams Approximation (WWA). The WWA has a lot of advantages such as providing the skill to reach crude numerical predictions via simple formulae. In addition, it may principally ease the experimental analysis because it enables one to directly achieve a rough cross section for $\gamma^*\gamma^* \rightarrow X$ process via the examination of the main process $e^-e^+ \rightarrow e^-Xe^+$ where X represents objects produced in the final state. The production of high mass objects is particularly interesting at the linear colliders and the production rate of massive objects is limited by the photon luminosity at high invariant mass while $\gamma^*\gamma^*$ and $e\gamma^*$ processes at the linear colliders arise from quasireal photon emitted from the incoming beams. Hence, $\gamma^*\gamma^*$ and $e\gamma^*$ are more realistic than $\gamma\gamma$ and $e\gamma$. These processes have been observed experimentally at LEP, Tevatron and LHC [30–64].

In this paper, we perform a phenomenological study for determining the sensitivity on the magnetic moment and electric dipole moment of the top quark through the $t\bar{t}$ pair production in e^+e^- colliders, specifically for center-of-mass energy and luminosity of CLIC-1.4 TeV, $\mathcal{L} = 1500 \text{ bf}^{-1}$ and CLIC-3 TeV, $\mathcal{L} = 2000 \text{ bf}^{-1}$ with systematic uncertainty of $\delta_{sys} = 0, 5, 10 \%$ and 95% C.L.. Here, we consider that the top quark pair production in e^+e^- interactions are given through three different processes $\gamma\gamma \rightarrow t\bar{t}$, $e\gamma \rightarrow e\gamma^*\gamma \rightarrow et\bar{t}$, $e^-e^+ \rightarrow e^-\gamma^*\gamma^*e^+ \rightarrow e^-t\bar{t}e^+$ where γ and γ^* are Compton backscattered and Weizsacker-Williams photons, respectively. These processes are one of the most important sources of $t\bar{t}$ pair production and may represent new physics effects at a high energy and high luminosity linear electron positron collider such as the CLIC and also isolate anomalous $t\bar{t}\gamma$ coupling from $t\bar{t}Z$.

This work is structured as follows. In Section II, we introduce the top quark effective electromagnetic interactions. In Section III, we study the dipole moments of the top quark through the processes $\gamma\gamma \rightarrow t\bar{t}$, $e\gamma \rightarrow e\gamma^*\gamma \rightarrow et\bar{t}$ and $e^-e^+ \rightarrow e^-\gamma^*\gamma^*e^+ \rightarrow e^-t\bar{t}e^+$. Finally,

we present our conclusions in Section IV.

II. TOP QUARK PAIR PRODUCTION PROCESSES IN PHOTON-PHOTON COLLISIONS

A. General Effective Coupling $t\bar{t}\gamma$

The most general effective coupling $t\bar{t}\gamma$ which includes the SM coupling and contributions from dimension-six effective operators can be written as [6, 9, 65–67]:

$$\mathcal{L}_{t\bar{t}\gamma} = -g_e Q_t \bar{t} \Gamma_{t\bar{t}\gamma}^\mu t A_\mu, \quad (1)$$

where g_e is the electromagnetic coupling constant, Q_t is the top quark electric charge and the Lorentz-invariant vertex function $\Gamma_{t\bar{t}\gamma}^\mu$, which describes the interaction of a γ photon with two top quarks, can be parameterized by

$$\Gamma_{t\bar{t}\gamma}^\mu = \gamma^\mu + \frac{i}{2m_t} (\hat{a}_V + i\hat{a}_A \gamma_5) \sigma^{\mu\nu} q_\nu, \quad (2)$$

where m_t is the mass of the top quark, q is the momentum transfer to the photon and the couplings \hat{a}_V and \hat{a}_A are real and related to the anomalous magnetic moment and the electric dipole moment of the top quark, respectively.

B. Theoretical Calculations

Schematic diagrams for the processes $e\gamma \rightarrow e\gamma^*\gamma \rightarrow e t\bar{t}$ and $e^-e^+ \rightarrow e^-\gamma^*\gamma^*e^+ \rightarrow e^-t\bar{t}e^+$ are given in Fig. 1. With these processes, $\gamma(\gamma^*)\gamma(\gamma^*) \rightarrow t\bar{t}$ have two Feynman diagrams which are shown in detail in Fig. 2.

For $\gamma\gamma$, $\gamma\gamma^*$ and $\gamma^*\gamma^*$ collisions including the effective Lagrangian in Eq. 1, the polarization summed amplitude square is given in function of the Mandelstam invariants \hat{s} , \hat{t} and \hat{u} as follows,

$$\begin{aligned}
|M_1|^2 = & \frac{16\pi^2 Q_t^2 \alpha_e^2}{2m_t^4 (\hat{t} - m_t^2)^2} \left[48\hat{a}_V(m_t^2 - \hat{t})(m_t^2 + \hat{s} - \hat{t})m_t^4 - 16(3m_t^4 - m_t^2\hat{s} + \hat{t}(\hat{s} + \hat{t}))m_t^4 \right. \\
& + 2(m_t^2 - \hat{t})(\hat{a}_V^2(17m_t^4 + (22\hat{s} - 26\hat{t})m_t^2 + \hat{t}(9\hat{t} - 4\hat{s}))) \\
& + \hat{a}_A^2(17m_t^2 + 4\hat{s} - 9\hat{t})(m_t^2 - \hat{t})m_t^2 + 12\hat{a}_V(\hat{a}_V^2 + \hat{a}_A^2)\hat{s}(m_t^3 - m_t\hat{t})^2 \\
& \left. - (\hat{a}_V^2 + \hat{a}_A^2)^2(m_t^2 - \hat{t})^3(m_t^2 - \hat{s} - \hat{t}) \right], \tag{3}
\end{aligned}$$

$$\begin{aligned}
|M_2|^2 = & \frac{-16\pi^2 Q_t^2 \alpha_e^2}{2m_t^4 (\hat{u} - m_t^2)^2} \left[48\hat{a}_V(m_t^4 + (\hat{s} - 2\hat{t})m_t^2 + \hat{t}(\hat{s} + \hat{t}))m_t^4 \right. \\
& + 16(7m_t^4 - (3\hat{s} + 4\hat{t})m_t^2 + \hat{t}(\hat{s} + \hat{t}))m_t^4 \\
& + 2(m_t^2 - \hat{t})(\hat{a}_V^2(m_t^4 + (17\hat{s} - 10\hat{t})m_t^2 + 9\hat{t}(\hat{s} + \hat{t}))) \\
& + \hat{a}_A^2(m_t^2 - 9\hat{t})(m_t^2 - \hat{t} - \hat{s})m_t^2 \\
& \left. + (\hat{a}_V^2 + \hat{a}_A^2)^2(m_t^2 - \hat{t})^3(m_t^2 - \hat{s} - \hat{t}) \right], \tag{4}
\end{aligned}$$

$$\begin{aligned}
M_1^\dagger M_2 + M_2^\dagger M_1 = & \frac{16\pi^2 Q_t^2 \alpha_e^2}{m_t^2 (\hat{t} - m_t^2)(\hat{u} - m_t^2)} \\
& \times \left[-16(4m_t^6 - m_t^4\hat{s}) + 8\hat{a}_V m_t^2(6m_t^4 - 6m_t^2(\hat{s} + 2\hat{t}) - \hat{s})^2 \right. \\
& + 6\hat{t})^2 + 6\hat{s}\hat{t}) + (\hat{a}_V^2(16m_t^6 - m_t^4(15\hat{s} + 32\hat{t}) + m_t^2(15\hat{s})^2 \\
& + 14\hat{t}\hat{s} + 16\hat{t})^2) + \hat{s}\hat{t}(\hat{s} + \hat{t})) + \hat{a}_A^2(16m_t^6 - m_t^4(15\hat{s} + 32\hat{t}) \\
& + m_t^2(5\hat{s})^2 + 14\hat{t}\hat{s} + 16\hat{t})^2) + \hat{s}\hat{t}(\hat{s} + \hat{t})) - 4\hat{a}_V\hat{s}(\hat{a}_V^2 + \hat{a}_A^2) \\
& \times (m_t^4 + m_t^2(\hat{s} - 2\hat{t}) + \hat{t}(\hat{s} + \hat{t})) - 4\hat{a}_A(\hat{a}_V^2 + \hat{a}_A^2)(2m_t^2 - \hat{s} - 2\hat{t}) \\
& \left. \times \epsilon_{\alpha\beta\gamma\delta} p_1^\alpha p_2^\beta p_3^\gamma p_4^\delta - 2\hat{s}(\hat{a}_V^2 + \hat{a}_A^2)^2(m_t^4 - 2\hat{t}m_t^2 + \hat{t}(\hat{s} + \hat{t})) \right], \tag{5}
\end{aligned}$$

where $\hat{s} = (p_1 + p_2)^2 = (p_3 + p_4)^2$, $\hat{t} = (p_1 - p_3)^2 = (p_4 - p_2)^2$, $\hat{u} = (p_3 - p_2)^2 = (p_1 - p_4)^2$ and p_1 and p_2 are the four-momenta of the incoming photons, p_3 and p_4 are the momenta of the outgoing top quarks, Q_t is the top quark charge, $\alpha_e = g_e^2/4\pi$ is the fine-structure constant, m_t is the mass of top and \hat{a}_V (\hat{a}_A) are their dipole moments.

The most promising mechanism to generate energetic photon beams in a linear collider is Compton backscattering. Compton backscattered photons interact with each other and generate the process $\gamma\gamma \rightarrow t\bar{t}$. The spectrum of Compton backscattered photons is given by

$$f_\gamma(y) = \frac{1}{g(\zeta)} \left[1 - y + \frac{1}{1-y} - \frac{4y}{\zeta(1-y)} + \frac{4y^2}{\zeta^2(1-y)^2} \right], \quad (6)$$

where

$$g(\zeta) = \left(1 - \frac{4}{\zeta} - \frac{8}{\zeta^2} \right) \log(\zeta + 1) + \frac{1}{2} + \frac{8}{\zeta} - \frac{1}{2(\zeta + 1)^2}, \quad (7)$$

with

$$y = \frac{E_\gamma}{E_e}, \quad \zeta = \frac{4E_0E_e}{M_e^2}, \quad y_{max} = \frac{\zeta}{1+\zeta}. \quad (8)$$

Here, E_0 and E_e are energy of the incoming laser photon and initial energy of the electron beam before Compton backscattering and E_γ is the energy of the backscattered photon. The maximum value of y reaches 0.83 when $\zeta = 4.8$.

WWA is another possibility for top pair production. The quasireal photons emitted from both lepton beams collide with each other and produce the process $\gamma^*\gamma^* \rightarrow t\bar{t}$. In WWA, the photon spectrum is given by

$$f_{\gamma^*}(x) = \frac{\alpha}{\pi E_e} \left\{ \left[\frac{1-x+x^2/2}{x} \right] \log\left(\frac{Q_{max}^2}{Q_{min}^2}\right) - \frac{m_e^2 x}{Q_{min}^2} \left(1 - \frac{Q_{min}^2}{Q_{max}^2} \right) - \frac{1}{x} \left[1 - \frac{x}{2} \right]^2 \log\left(\frac{x^2 E_e^2 + Q_{max}^2}{x^2 E_e^2 + Q_{min}^2}\right) \right\} \quad (9)$$

where $x = E_\gamma/E_e$ and Q_{max}^2 is maximum virtuality of the photon. In this work, we have taken into account the maximum virtuality of the photon is $Q_{max}^2 = 2 \text{ GeV}^2$. The larger values of Q_{max}^2 do not make a significant contribution to the sensitivity limits which is similar to results in previous works [68–71]. The minimum value of the Q_{min}^2 is given by

$$Q_{min}^2 = \frac{m_e^2 x^2}{1-x}. \quad (10)$$

The Q_{min}^2 value is very small due to the electron mass. However, the scattering angles of the electrons are so small that the transverse momentum is close to zero. Due to the momentum conservation, the transverse momentum of the emitted photons also have small values. In light of all these arguments, virtuality of the photons in WWA is very small and the photons are almost on mass shell.

The process $\gamma^*\gamma^* \rightarrow t\bar{t}$ participates as a subprocess in the main process $e^-e^+ \rightarrow e^-\gamma^*\gamma^*e^+ \rightarrow e^-t\bar{t}e^+$. However, an γ^* photon emitted from either of the incoming leptons can interact with the Compton backscattered photon and the subprocess $\gamma\gamma^* \rightarrow t\bar{t}$ can take place. Hence, we calculate the process $e\gamma \rightarrow e\gamma^*\gamma \rightarrow et\bar{t}$ by integrating the cross section for the subprocess $\gamma\gamma^* \rightarrow t\bar{t}$.

The total cross sections are,

$$\sigma = \int f_{\gamma(\gamma^*)}(x)f_{\gamma(\gamma^*)}(x)d\hat{\sigma}dE_1dE_2. \quad (11)$$

The total cross sections of these processes as functions of anomalous \hat{a}_V and \hat{a}_A are shown in Figs. 3-5. In these figures, the cross sections depending on the anomalous couplings were obtained by varying only one of the anomalous couplings at a time while the other was fixed to zero. We understand from Figs. 3-5 that the total cross sections show a clear dependence on the dipole moments of the top quark. Anomalous \hat{a}_V and \hat{a}_A parameters have different CP properties which can be seen in Eqs. 3-5. The cross section with respect to the \hat{a}_A parameter is even power and a nonzero value of this parameter allows a constructive effect on the total cross section. In addition, the contribution of \hat{a}_V coupling to the cross sections is proportional to odd power. In Fig. 3, there are small intervals around \hat{a}_V in which the cross section that includes new physics is smaller than the SM cross section. For this reason, the \hat{a}_V parameter has a partially destructive effect on the total cross section.

When comparing the three processes in Figs. 3-5, the largest deviation from the SM of the anomalous cross sections, including anomalous \hat{a}_V and \hat{a}_A couplings, is the process $\gamma\gamma \rightarrow t\bar{t}$. Therefore, the best sensitivities on anomalous \hat{a}_V and \hat{a}_A couplings are obtained from the process $\gamma\gamma \rightarrow t\bar{t}$. Similarly, the sensitivities obtained on anomalous couplings through the process $e\gamma \rightarrow e\gamma^*\gamma \rightarrow et\bar{t}$ are expected to be more restrictive than the sensitivities on the process $e^-e^+ \rightarrow e^-\gamma^*\gamma^*e^+ \rightarrow e^-t\bar{t}e^+$.

When making a direct comparison of our results for the total cross section as a function of the dipole moments \hat{a}_V and \hat{a}_A reported in Figs. 3-5 with those reported in Ref. [9] (see Figs. 3-4), we find that our results, using processes $\gamma\gamma \rightarrow t\bar{t}$, $\gamma\gamma^* \rightarrow t\bar{t}$ and $\gamma^*\gamma^* \rightarrow t\bar{t}$ at CLIC energies, with respect to process $pp \rightarrow p\gamma^*\gamma^*p \rightarrow pt\bar{t}p$ at LHC energies, show a significant improvement. In addition, with our processes the total cross sections are of 3-4 orders of magnitude better than those reported in Ref. [9]. This shows that the bounds on the anomalous couplings \hat{a}_V and \hat{a}_A can be improved at a linear collider such as the CLIC

by a few orders of magnitude when compared to what is possible at the LHC.

III. DIPOLE MOMENTS OF THE TOP QUARK IN $\gamma\gamma$, $\gamma\gamma^*$ AND $\gamma^*\gamma^*$ COLLISIONS

To investigate the sensitivity to the anomalous \hat{a}_V and \hat{a}_A couplings we use the chi-squared distribution:

$$\chi^2 = \left(\frac{\sigma_{SM} - \sigma_{NP}(\hat{a}_V, \hat{a}_A)}{\sigma_{SM}\delta} \right)^2, \quad (12)$$

where $\sigma_{NP}(\hat{a}_V, \hat{a}_A)$ is the total cross section including contributions from the SM and New physics, $\delta = \sqrt{(\delta_{st})^2 + (\delta_{sys})^2}$, $\delta_{st} = \frac{1}{\sqrt{N_{SM}}}$ is the statistical error and δ_{sys} is the systematic error. The number of events for each of the three processes is given by $N_{SM} = \mathcal{L}_{int} \times BR \times \sigma_{SM} \times \epsilon_{b-tag} \times \epsilon_{b-tag}$, where \mathcal{L}_{int} is the integrated luminosity and b-jet tagging efficiency is 0.8 [72]. The top quarks decay almost 100% to W boson and b quark. For top quark pair production we can categorize decay products according to the decomposition of W . In this work, we assume that one of the W bosons decays leptonically and the other hadronically for the signal. This phenomenon has already been studied by ATLAS and CMS Collaborations [73–75]. Thus, we assume that the branching ratio of the top quark pair in the final state to be $BR = 0.286$.

For our numerical computation, we take a set of independent input parameters which are known from current experiments. The input parameters are $\alpha = \frac{1}{137.4}$, $m_b = 4.18 \text{ GeV}$, $m_t = 173.21 \text{ GeV}$ [76] and for our analysis, we consider a 95% C.L. sensitivity on the dipole moments \hat{a}_V and \hat{a}_A of the top quark via the processes $\gamma\gamma \rightarrow t\bar{t}$, $e\gamma \rightarrow e\gamma^*\gamma \rightarrow et\bar{t}$ and $e^-e^+ \rightarrow e^-\gamma^*\gamma^*e^+ \rightarrow e^-t\bar{t}e^+$ at the CLIC-1.4 TeV with $\mathcal{L}_{int} = 1500 \text{ fb}^{-1}$ and CLIC-3 TeV with $\mathcal{L}_{int} = 2000 \text{ fb}^{-1}$.

Tables I-VI illustrate the sensitivity obtained at 95% *C.L.* on the dipole moments \hat{a}_V and \hat{a}_A of the top quark through the processes $\gamma\gamma \rightarrow t\bar{t}$, $e\gamma \rightarrow e\gamma^*\gamma \rightarrow et\bar{t}$ and $e^-e^+ \rightarrow e^-\gamma^*\gamma^*e^+ \rightarrow e^-t\bar{t}e^+$. The bounds are obtained assuming that the center-of-mass energy of CLIC-1.4 TeV and luminosities of $\mathcal{L} = 50, 300, 500, 1000, 1500 \text{ fb}^{-1}$ for the second stage of operation of the collider. For the third stage, we consider the center-of-mass energy of CLIC-3 TeV and luminosities of $\mathcal{L} = 50, 300, 500, 1000, 1500, 2000 \text{ fb}^{-1}$.

An important part of our analysis is the inclusion of theoretical uncertainties as there

may be several experimental and systematic uncertainty sources in top quark identification. This situation has not been studied experimentally in linear colliders. For hadron colliders, especially LHC, the process of determining the cross section of top pair production has been experimentally studied [77, 78]. As seen from these studies, the total systematic uncertainty value is about 10% and is increasingly improved when it is compared with previous experimental studies [75].

We use three scenarios for the systematic uncertainties in our entire set of Tables: (1) we assume a systematic uncertainty of $\delta_{sys} = 0\%$, (2) we estimate future results for \hat{a}_V and \hat{a}_A with 5% systematic uncertainty and (3) we consider a systematic uncertainty of as much as $\delta_{sys} = 10\%$. We find in Tables I-VI that the most prominent mode of top quark pair production that imposes stronger limits on the dipole moments is the production process $\gamma\gamma \rightarrow t\bar{t}$, followed in order of importance by the processes $e\gamma \rightarrow e\gamma^*\gamma \rightarrow et\bar{t}$ and $e^-e^+ \rightarrow e^-\gamma^*\gamma^*e^+ \rightarrow e^-t\bar{t}e^+$, respectively. In conclusion, it is possible that the CLIC may put limits on the electromagnetic dipole moments of the top quark with a sensitivity of the order $\mathcal{O}(10^{-3} - 10^{-2})$ at the 95% *C.L.*. We can see from the Figs 3-5, the cross section for the negative values of the \hat{a}_v are smaller than their positive values. This can easily be seen on sensitivity tables: the bounds for the negative values of the \hat{a}_v for increasing luminosity values do not change much.

It is worthwhile to compare the results obtained here with those of Ref. [9] which consider the process $pp \rightarrow p\gamma^*\gamma^*p \rightarrow pt\bar{t}p$ with the LHC running at $\sqrt{s} = 14, 33 \text{ TeV}$ and with integrated luminosities of $\mathcal{L} = 100, 300, 3000 \text{ fb}^{-1}$. Varying one coupling at a time, they find constraints at 68% *C.L.* of the order $\mathcal{O}(10^{-2} - 10^{-1})$. We also note that, while we do consider three systematic errors in our study, the quoted sensitivities in Ref. [9] do not include theoretical uncertainty. Also, the CLIC sensitivity is even better for our processes than for those reported in Ref. [9].

Finally, in Figs. 6-8 we show the 95% C.L. contours for anomalous $\hat{a}_V - \hat{a}_A$ couplings for the processes $\gamma\gamma \rightarrow t\bar{t}$, $e\gamma \rightarrow e\gamma^*\gamma \rightarrow et\bar{t}$ and $e^-e^+ \rightarrow e^-\gamma^*\gamma^*e^+ \rightarrow e^-t\bar{t}e^+$ at the CLIC for various integrated luminosities and center-of-mass energies. Among the three combinations shown in these figures, we find that the strongest simultaneous limits come from the reaction $\gamma\gamma \rightarrow t\bar{t}$ at the CLIC-3 *TeV* and $\mathcal{L}_{int} = 2000 \text{ fb}^{-1}$ with the 3σ level.

IV. CONCLUSIONS

The LHC is expected to provide answers to some fundamental questions of the SM. However, high precision measurements may not be available due to remnants from the strong interactions of proton-proton collisions. For this reason, the linear collider with high luminosity and energy is a good choice to complement and extend the LHC physics program. This collider with high luminosity and energy is extremely important to examine new physics beyond the SM. The anomalous $t\bar{t}\gamma$ coupling have very strong energy dependencies since they are characterized by effective Lagrangians that contains dimensional-high operators. Thus, the cross section including the anomalous $t\bar{t}\gamma$ coupling has a higher energy dependence than the SM cross section. The anomalous $t\bar{t}\gamma$ coupling can be analyzed through the process $e^-e^+ \rightarrow t\bar{t}$ at the linear colliders. This process receives contributions from both anomalous $t\bar{t}\gamma$ and $t\bar{t}Z$ couplings. However, the processes $\gamma\gamma \rightarrow t\bar{t}$, $e\gamma \rightarrow e\gamma^*\gamma \rightarrow et\bar{t}$ and $e^-e^+ \rightarrow e^-\gamma^*\gamma^*e^+ \rightarrow e^-t\bar{t}e^+$ isolate $t\bar{t}\gamma$ coupling which provides the possibility to analyze the $t\bar{t}\gamma$ coupling separately from the $t\bar{t}Z$ coupling. Any signal which conflicts with the SM predictions would be convincing evidence for new physics effects in $t\bar{t}\gamma$.

In this paper, we carry out a phenomenological study to investigate the sensitivity of the CLIC to the anomalous $t\bar{t}\gamma$ coupling through the $\gamma\gamma$, $\gamma\gamma^*$ and $\gamma^*\gamma^*$ collision modes followed by the semileptonic decay of the top pair production. We find that with a center-of-mass energy of CLIC-1.4 TeV, integrated luminosity of $\mathcal{L} = 1500 fb^{-1}$ and CLIC-3 TeV and integrated luminosity of $\mathcal{L} = 2000 fb^{-1}$ with systematic uncertainties of $\delta_{sys} = 0, 5, 10\%$ at the 95% C.L., it is possible that the CLIC may put limits on the electromagnetic dipole moments of the top quark \hat{a}_V and \hat{a}_A with a sensitivity of the order $\mathcal{O}(10^{-3} - 10^{-2})$. In addition, it is noteworthy that our bounds on the dipole moments of the top quark \hat{a}_V and \hat{a}_A at 1σ are predicted to be of the order $\mathcal{O}(10^{-4} - 10^{-3})$, which is an order of magnitude better than those reported in Refs. [10–21]. Finally, we highlight that the sensitivity with the CLIC data is much stronger than that reported in the literature for the LHC [16] and the ILC [14, 15, 18] data. In conclusion, despite the fact that the LHC prospects are already strong due to its excellent statistic, the sensitivity of ILC and the CLIC is even stronger.

TABLE I: Sensitivity on the \hat{a}_V magnetic moment and the \hat{a}_A electric dipole moment for the process $\gamma\gamma \rightarrow t\bar{t}$.

| 95% C.L. | | | | |
|------------------|-------------------------|----------------|-------------------|---------------|
| $\sqrt{s} (TeV)$ | $\mathcal{L} (fb^{-1})$ | δ_{sys} | \hat{a}_V | $ \hat{a}_A $ |
| 1.4 | 50 | 0% | [-0.5277, 0.0104] | 0.0685 |
| 1.4 | 50 | 5% | [-0.5668, 0.0359] | 0.1309 |
| 1.4 | 50 | 10% | [-0.6130, 0.0646] | 0.1820 |
| 1.4 | 300 | 0% | [-0.5184, 0.0043] | 0.0438 |
| 1.4 | 300 | 5% | [-0.5651, 0.0348] | 0.1288 |
| 1.4 | 300 | 10% | [-0.6123, 0.0641] | 0.1812 |
| 1.4 | 500 | 0% | [-0.5170, 0.0034] | 0.0385 |
| 1.4 | 500 | 5% | [-0.5650, 0.0347] | 0.1286 |
| 1.4 | 500 | 10% | [-0.6122, 0.0641] | 0.1811 |
| 1.4 | 1000 | 0% | [-0.5155, 0.0024] | 0.0324 |
| 1.4 | 1000 | 5% | [-0.5649, 0.0346] | 0.1285 |
| 1.4 | 1000 | 10% | [-0.6122, 0.0641] | 0.1811 |
| 1.4 | 1500 | 0% | [-0.5149, 0.0020] | 0.0293 |
| 1.4 | 1500 | 5% | [-0.5648, 0.0346] | 0.1284 |
| 1.4 | 1500 | 10% | [-0.6121, 0.0640] | 0.1811 |

Acknowledgments

A. G. R. acknowledges support from CONACyT, SNI and PROFOCIE (México).

-
- [1] W. Bernreuther, R. Bonciani, T. Gehrmann, R. Heinesch, T. Leineweber, P. Mastrolia, E. Remiddi, *Phys. Rev. Lett.* **95**, 261802 (2005).
- [2] F. Hoogeveen, *Nucl. Phys.* **B341**, 322 (1990).
- [3] M. E. Pospelov and I. B. Khriplovich, *Sov. J. Nucl. Phys.* **53**, 638 (1991) [*Yad. Fiz.* 53 (1991) 1030].

TABLE II: Sensitivity on the \hat{a}_V magnetic moment and the \hat{a}_A electric dipole moment for the process $\gamma\gamma \rightarrow t\bar{t}$.

| 95% C.L. | | | | |
|------------------|-------------------------|----------------|-------------------|---------------|
| $\sqrt{s} (TeV)$ | $\mathcal{L} (fb^{-1})$ | δ_{sys} | \hat{a}_V | $ \hat{a}_A $ |
| 3 | 50 | 0% | [-0.2320, 0.0122] | 0.0517 |
| 3 | 50 | 5% | [-0.2581, 0.0345] | 0.0914 |
| 3 | 50 | 10% | [-0.2877, 0.0590] | 0.1262 |
| 3 | 300 | 0% | [-0.2239, 0.0052] | 0.0330 |
| 3 | 300 | 5% | [-0.2565, 0.0332] | 0.0894 |
| 3 | 300 | 10% | [-0.2870, 0.0586] | 0.1255 |
| 3 | 500 | 0% | [-0.2225, 0.0040] | 0.0291 |
| 3 | 500 | 5% | [-0.2564, 0.0331] | 0.0892 |
| 3 | 500 | 10% | [-0.2870, 0.0585] | 0.1254 |
| 3 | 1000 | 0% | [-0.2212, 0.0029] | 0.0245 |
| 3 | 1000 | 5% | [-0.2563, 0.0330] | 0.0891 |
| 3 | 1000 | 10% | [-0.2869, 0.0585] | 0.1254 |
| 3 | 1500 | 0% | [-0.2206, 0.0024] | 0.0221 |
| 3 | 1500 | 5% | [-0.2563, 0.0330] | 0.0890 |
| 3 | 1500 | 10% | [-0.2869, 0.0585] | 0.1254 |
| 3 | 2000 | 0% | [-0.2203, 0.0020] | 0.0206 |
| 3 | 2000 | 5% | [-0.2563, 0.0330] | 0.0879 |
| 3 | 2000 | 10% | [-0.2869, 0.0585] | 0.1254 |

- [4] A. Soni and R. M. Xu, *Phys. Rev. Lett.* **69**, 33 (1992).
- [5] T. Ibrahim and P. Nath, *Phys. Rev.* **D82**, 055001 (2010).
- [6] U. Baur, A. Juste, L. H. Orr and D. Rainwater, *Phys. Rev.* **D71**, 054013 (2005).
- [7] A. O. Bouzas and F. Larios, *Phys. Rev.* **D87**, 074015 (2013).
- [8] A. O. Bouzas and F. Larios, *Phys. Rev.* **D88**, 094007 (2013).
- [9] Sh. Fayazbakhsh, S. Taheri Monfared and M. Mohammadi Najafabadi, *Phys. Rev.* **D92**,

TABLE III: Sensitivity on the \hat{a}_V magnetic moment and the \hat{a}_A electric dipole moment for the process $e\gamma \rightarrow e\gamma^*\gamma \rightarrow et\bar{t}$.

| 95% C.L. | | | | |
|------------------|-------------------------|----------------|-------------------|---------------|
| $\sqrt{s} (TeV)$ | $\mathcal{L} (fb^{-1})$ | δ_{sys} | \hat{a}_V | $ \hat{a}_A $ |
| 1.4 | 50 | 0% | [-0.7724, 0.0361] | 0.1504 |
| 1.4 | 50 | 5% | [-0.7942, 0.0482] | 0.1759 |
| 1.4 | 50 | 10% | [-0.8367, 0.0713] | 0.2185 |
| 1.4 | 300 | 0% | [-0.7360, 0.0154] | 0.0963 |
| 1.4 | 300 | 5% | [-0.7737, 0.0369] | 0.1521 |
| 1.4 | 300 | 10% | [-0.8253, 0.0652] | 0.2078 |
| 1.4 | 500 | 0% | [-0.7300, 0.0121] | 0.0848 |
| 1.4 | 500 | 5% | [-0.7717, 0.0358] | 0.1496 |
| 1.4 | 500 | 10% | [-0.8244, 0.0647] | 0.2068 |
| 1.4 | 1000 | 0% | [-0.7241, 0.0086] | 0.0713 |
| 1.4 | 1000 | 5% | [-0.7701, 0.0349] | 0.1477 |
| 1.4 | 1000 | 10% | [-0.8236, 0.0643] | 0.2061 |
| 1.4 | 1500 | 0% | [-0.7215, 0.0070] | 0.0644 |
| 1.4 | 1500 | 5% | [-0.7697, 0.0346] | 0.1470 |
| 1.4 | 1500 | 10% | [-0.8234, 0.0641] | 0.2059 |

014006 (2015).

- [10] D. Atwood, A. Aeppli and A. Soni, *Phys. Rev. Lett.* **69**, 2754 (1992).
- [11] P. Poulose and S. D. Rindani, *Phys. Rev.* **D57**, 5444 (1998) [Erratum-ibid. **D61**, 119902 (2000)].
- [12] S. Y. Choi and K. Hagiwara, *Phys. Lett.* **B359**, 369 (1995).
- [13] P. Poulose and S. D. Rindani, *Phys. Rev.* **D91**, 093008 (2015).
- [14] J. A. Aguilar-Saavedra, *et al.*, [TESLA: The Superconducting electron positron linear collider with an integrated x-ray laser laboratory. Technical design report. Part 3. Physics at an e^+e^- linear collider], arXiv:hep-ph/0106315, and references therein.

TABLE IV: Sensitivity on the \hat{a}_V magnetic moment and the \hat{a}_A electric dipole moment for the process $e\gamma \rightarrow e\gamma^*\gamma \rightarrow et\bar{t}$.

| 95% C.L. | | | | |
|------------------|-------------------------|----------------|-------------------|---------------|
| $\sqrt{s} (TeV)$ | $\mathcal{L} (fb^{-1})$ | δ_{sys} | \hat{a}_V | $ \hat{a}_A $ |
| 3 | 50 | 0% | [-0.4855, 0.0267] | 0.1083 |
| 3 | 50 | 5% | [-0.5054, 0.0419] | 0.1383 |
| 3 | 50 | 10% | [-0.5380, 0.0664] | 0.1795 |
| 3 | 300 | 0% | [-0.4658, 0.0113] | 0.0692 |
| 3 | 300 | 5% | [-0.4970, 0.0354] | 0.1260 |
| 3 | 300 | 10% | [-0.5337, 0.0632] | 0.1745 |
| 3 | 500 | 0% | [-0.4626, 0.0088] | 0.0610 |
| 3 | 500 | 5% | [-0.4961, 0.0034] | 0.1249 |
| 3 | 500 | 10% | [-0.5333, 0.0630] | 0.1740 |
| 3 | 1000 | 0% | [-0.4593, 0.0063] | 0.0512 |
| 3 | 1000 | 5% | [-0.4955, 0.0343] | 0.1240 |
| 3 | 1000 | 10% | [-0.5332, 0.0629] | 0.1737 |
| 3 | 1500 | 0% | [-0.4579, 0.0052] | 0.0463 |
| 3 | 1500 | 5% | [-0.4953, 0.0342] | 0.1237 |
| 3 | 1500 | 10% | [-0.5331, 0.0628] | 0.1736 |
| 3 | 2000 | 0% | [-0.4570, 0.0045] | 0.0431 |
| 3 | 2000 | 5% | [-0.4952, 0.0341] | 0.1236 |
| 3 | 2000 | 10% | [-0.5330, 0.0627] | 0.1735 |

- [15] M. Amjad, M. Boronat, T. Frisson, I. G. Garca, R. Pöschl, *et al.*, *A precise determination of top quark electro-weak couplings at the ILC operating at $\sqrt{s} = 500 GeV$* , arXiv:1307.8102 [hep-ex], and references therein.
- [16] A. Juste, Y. Kiyo, F. Petriello, T. Teubner, K. Agashe, *et al.*, *Report of the 2005 Snowmass top/QCD working group*, arXiv:hep-ph/0601112 [hep-ph], and references therein.
- [17] D. Asner, *et al.*, arXiv:1307.8265 [hep-ex] and references therein.

TABLE V: Sensitivity on the \hat{a}_V magnetic moment and the \hat{a}_A electric dipole moment for the process $e^-e^+ \rightarrow e^-\gamma^*\gamma^*e^+ \rightarrow e^-t\bar{t}e^+$

| 95% C.L. | | | | |
|------------------|-------------------------|----------------|-------------------|---------------|
| $\sqrt{s} (TeV)$ | $\mathcal{L} (fb^{-1})$ | δ_{sys} | \hat{a}_V | $ \hat{a}_A $ |
| 1.4 | 50 | 0% | [-1.085, 0.1328] | 0.3314 |
| 1.4 | 50 | 5% | [-1.0908, 0.1352] | 0.3350 |
| 1.4 | 50 | 10% | [-1.1050, 0.1410] | 0.3449 |
| 1.4 | 300 | 0% | [-0.9377, 0.0620] | 0.2132 |
| 1.4 | 300 | 5% | [-0.9514, 0.0688] | 0.2260 |
| 1.4 | 300 | 10% | [-0.9847, 0.0850] | 0.2548 |
| 1.4 | 500 | 0% | [-0.9123, 0.0490] | 0.1878 |
| 1.4 | 500 | 5% | [-0.9298, 0.0580] | 0.2057 |
| 1.4 | 500 | 10% | [-0.9690, 0.0774] | 0.2415 |
| 1.4 | 1000 | 0% | [-0.8859, 0.0357] | 0.1581 |
| 1.4 | 1000 | 5% | [-0.9090, 0.0478] | 0.1850 |
| 1.4 | 1000 | 10% | [-0.9558, 0.0709] | 0.2299 |
| 1.4 | 1500 | 0% | [-0.8739, 0.0295] | 0.1429 |
| 1.4 | 1500 | 5% | [-0.9014, 0.0437] | 0.1762 |
| 1.4 | 1500 | 10% | [-0.9510, 0.0686] | 0.2256 |

- [18] American Linear Collider Working Group Collaboration, T. Abe et al., *Linear Collider Physics Resource Book for Snowmass 2001 - Part 3*, arXiv:hep-ex/0106057 and references therein.
- [19] G. Aarons, *et al.*, [ILC Collaboration], arXiv:0709.1893 [hep-ph].
- [20] J. Brau, *et al.*, [ILC Collaboration], arXiv:0712.1950 [physics.acc-ph].
- [21] H. Baer, T. Barklow, K. Fujii, *et al.*, arXiv:1306.6352 [hep-ph].
- [22] M. Köksal, A. A. Billur and A. Gutiérrez-Rodríguez, Adv. High Energy Phys. 2017, 6738409 (2017).
- [23] H. Abramowicz, *et al.*, The CLIC Detector and Physics Study, arXiv:1307.5288 [hep-ex].
- [24] I. F. Ginzburg, arXiv:1508.06581 [hep-ph].

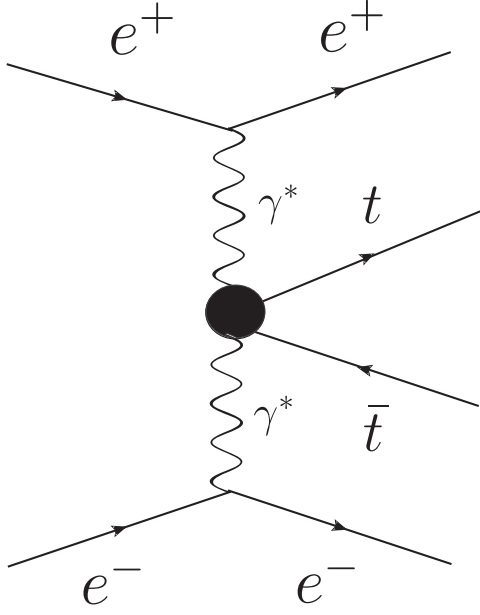
TABLE VI: Sensitivity on the \hat{a}_V magnetic moment and the \hat{a}_A electric dipole moment for the process $e^-e^+ \rightarrow e^-\gamma^*\gamma^*e^+ \rightarrow e^-t\bar{t}e^+$.

| 95% C.L. | | | | |
|------------------|-------------------------|----------------|-------------------|---------------|
| $\sqrt{s} (TeV)$ | $\mathcal{L} (fb^{-1})$ | δ_{sys} | \hat{a}_V | $ \hat{a}_A $ |
| 3 | 50 | 0% | [-0.6977, 0.0817] | 0.2225 |
| 3 | 50 | 5% | [-0.7044, 0.0862] | 0.2297 |
| 3 | 50 | 10% | [-0.7220, 0.0980] | 0.2477 |
| 3 | 300 | 0% | [-0.6320, 0.0370] | 0.1429 |
| 3 | 300 | 5% | [-0.6491, 0.0486] | 0.1660 |
| 3 | 300 | 10% | [-0.6816, 0.0709] | 0.2050 |
| 3 | 500 | 0% | [-0.6212, 0.0291] | 0.1259 |
| 3 | 500 | 5% | [-0.6417, 0.0434] | 0.1561 |
| 3 | 500 | 10% | [-0.6773, 0.0679] | 0.2000 |
| 3 | 1000 | 0% | [-0.6097, 0.0210] | 0.1059 |
| 3 | 1000 | 5% | [-0.6353, 0.0390] | 0.1472 |
| 3 | 1000 | 10% | [-0.6739, 0.0656] | 0.1962 |
| 3 | 1500 | 0% | [-0.6044, 0.0173] | 0.0957 |
| 3 | 1500 | 5% | [-0.6330, 0.0374] | 0.1439 |
| 3 | 1500 | 10% | [-0.6728, 0.0648] | 0.1948 |
| 3 | 2000 | 0% | [-0.6013, 0.0151] | 0.0890 |
| 3 | 2000 | 5% | [-0.6317, 0.0365] | 0.1420 |
| 3 | 2000 | 10% | [-0.6721, 0.0644] | 0.1942 |

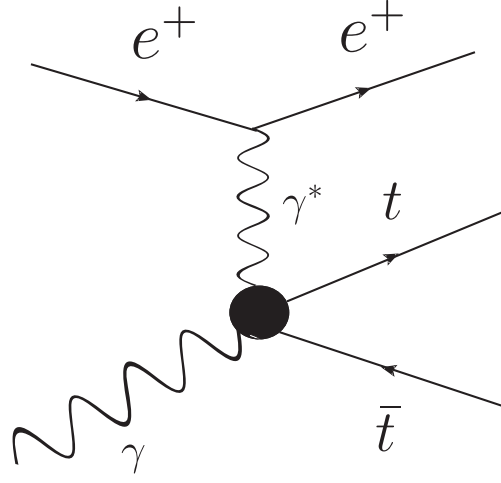
- [25] I. F. Ginzburg, G. L. Kotkin, S. L. Panfil, V. G. Serbo and V. I. Telnov, *Nucl. Instrum. Meth.* **A219**, 5 (1984).
- [26] S. J. Brodsky, T. Kinoshita and H. Terazawa, *Phys. Rev.* **D4**, 1532 (1971).
- [27] V. M. Budnev, I. F. Ginzburg, G. V. Meledin and V. G. Serbo, *Phys. Rep.* **15**, 181 (1975).
- [28] H. Terazawa, *Rev. Mod. Phys.* **45**, 615 (1973).
- [29] J. M. Yang, *Annals Phys.* **316**, 529 (2005).

- [30] A. Abulencia, *et al.*, [CDF Collaboration], *Phys. Rev. Lett.* **98**, 112001 (2007).
- [31] T. Aaltonen, *et al.*, [CDF Collaboration], *Phys. Rev. Lett.* **102**, 222002 (2009).
- [32] T. Aaltonen, *et al.*, [CDF Collaboration], *Phys. Rev. Lett.* **102**, 242001 (2009).
- [33] S. Chatrchyan, *et al.*, [CMS Collaboration], *JHEP* **1201**, 052 (2012).
- [34] S. Chatrchyan, *et al.*, [CMS Collaboration], *JHEP* **1211**, 080 (2012).
- [35] V. M. Abazov, *et al.*, [D0 Collaboration], *Phys. Rev.* **D88**, 012005 (2013).
- [36] S. Chatrchyan, *et al.*, [CMS Collaboration], *JHEP* **07**, 116 (2013).
- [37] S. C. Inan, *Phys. Rev.* **D81**, 115002 (2010).
- [38] S. C. Inan, *Nucl. Phys.* **B897**, 289 (2015).
- [39] S. C. Inan, *Int. J. Mod. Phys.* **A26**, 3605 (2011).
- [40] I. Sahin and S. C. Inan, *JHEP* **0909**, 069 (2009).
- [41] S. Atag, S. C. Inan and I. Sahin, *JHEP* **1009**, 042 (2010).
- [42] I. Sahin and B. Sahin, *Phys. Rev.* **D86**, 115001 (2012).
- [43] B. Sahin and A. A. Billur, *Phys. Rev.* **D86**, 074026 (2012).
- [44] A. Senol, *Int. J. Mod. Phys.* **A29**, 1450148 (2014).
- [45] A. Senol, *Phys. Rev.* **D87**, 073003 (2013).
- [46] S. Fichtel, G. von Gersdorff, B. Lenzi, C. Royon and M. Saimpert, *JHEP* **1502**, 165 (2015).
- [47] H. Sun, *Phys. Rev.* **D90**, 035018 (2014).
- [48] H. Sun, *Nucl. Phys.* **B886**, 691 (2014).
- [49] H. Sun, Y. J. Zhou and H. S. Hou, *JHEP* **1502**, 064 (2015).
- [50] A. Senol and M. Köksal, *JHEP* **1503**, 139 (2015).
- [51] S. Atag and A. A. Billur, *JHEP* **1011**, 060 (2010).
- [52] M. Köksal, V. Ari and A. Senol, *Adv. High Energy Phys.* **2016**, 8672391 (2016).
- [53] A. Senol and M. Köksal, *Phys. Lett. B* **742** (2015) 143.
- [54] M. Köksal and S. C. Inan, *Adv. High Energy Phys.* **2014** (2014) 935840.
- [55] M. Köksal, *Eur. Phys. J. Plus* **130** (2015) no.4, 75
- [56] A. A. Billur, *Europhys. Lett.* 101, 21001 (2013).
- [57] M. Köksal, *Int. J. Mod. Phys. A* 29, no. 24, 1450138 (2014).
- [58] M. Koksas, *Mod. Phys. Lett. A* 29, no. 34, 1450184 (2014).
- [59] V. Ari, A. A. Billur, S. C. Inan and M. Koksas, *Nucl. Phys. B* 906, 211 (2016).
- [60] M. Koksas and S. C. Inan, *Adv. High Energy Phys.* 2014, 315826 (2014).

- [61] I. Sahin and A. A. Billur, *Phys. Rev. D* **83**, 035011 (2011).
- [62] S. C. Inan and A. Billur, *Phys. Rev. D* **84**, 095002 (2011).
- [63] S. Fichet, *Acta Phys. Polon. Supp.* **8** (2015) 811.
- [64] H. Sun, Y. J. Zhou and H. S. Hou, *JHEP* **1502** (2015) 064.
- [65] J. F. Kamenik, M. Papucci and A. Weiler, *Phys. Rev.* **D85**, 071501 (2012).
- [66] J. A. Aguilar-Saavedra, *Nucl. Phys.* **B812**, 181 (2009).
- [67] J. A. Aguilar-Saavedra, M. C. N. Fiolhais and A. Onofre, *JHEP* **07**, 180 (2012).
- [68] A. A. Billur and M. Koksai, *Phys. Rev.* **D89**, no. 3, 037301 (2014).
- [69] A. Gutiérrez-Rodríguez, M. Koksai and A. A. Billur, *Phys. Rev.* **D91**, no. 9, 093008 (2015).
- [70] A. Gutiérrez-Rodríguez, M. Koksai and A. A. Billur, *PoS EPS-HEP2015*, 036 (2015), C15-07-22 Proceedings.
- [71] S. Atag and E. Gurkanlı, *JHEP* **1606**, 118 (2016).
- [72] ATLAS Collaboration, ATL-PHYS-PUB-2015-39.
- [73] ATLAS Collaboration, *Eur. Phys. J.* **C71**, 1577 (2011).
- [74] CMS Collaboration, CMS Collaboration, *Phys. Lett.* **B695**, 424 (2011).
- [75] CMS Collaboration, *Eur. Phys. J.* **C71**, 1721 (2011).
- [76] K. A. Olive, *et al.*, [Particle Data Group], *Chin. Phys.* **C38**, 090001 (2014).
- [77] ATLAS Collaboration, *Phys. Lett.* **B761**, 136 (2016).
- [78] V. Khachatryan, *et al.* (CMS Collaboration), *Phys. Rev. Lett.* **116**, 052002 (2016).

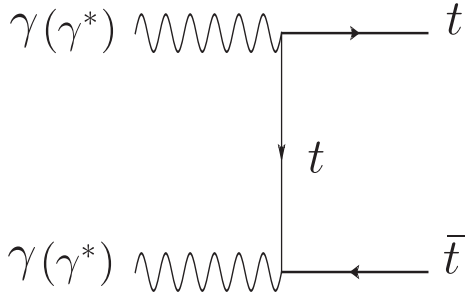


(a)

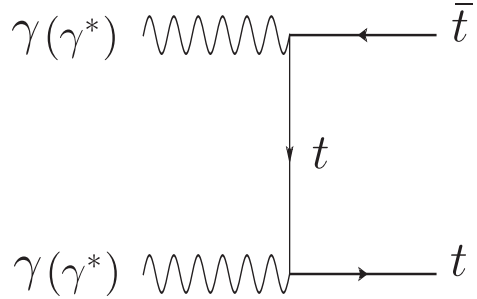


(b)

FIG. 1: A schematic diagram for the process (a) $e^-e^+ \rightarrow e^-\gamma^*\gamma^*e^+ \rightarrow e^-t\bar{t}e^+$ and (b) $e^+\gamma \rightarrow e^+\gamma^*\gamma \rightarrow e^+t\bar{t}$.



(a)



(b)

FIG. 2: Feynman diagrams contributing to the process $\gamma\gamma \rightarrow t\bar{t}$ and the subprocesses $\gamma\gamma^* \rightarrow t\bar{t}$ and $\gamma^*\gamma^* \rightarrow t\bar{t}$.

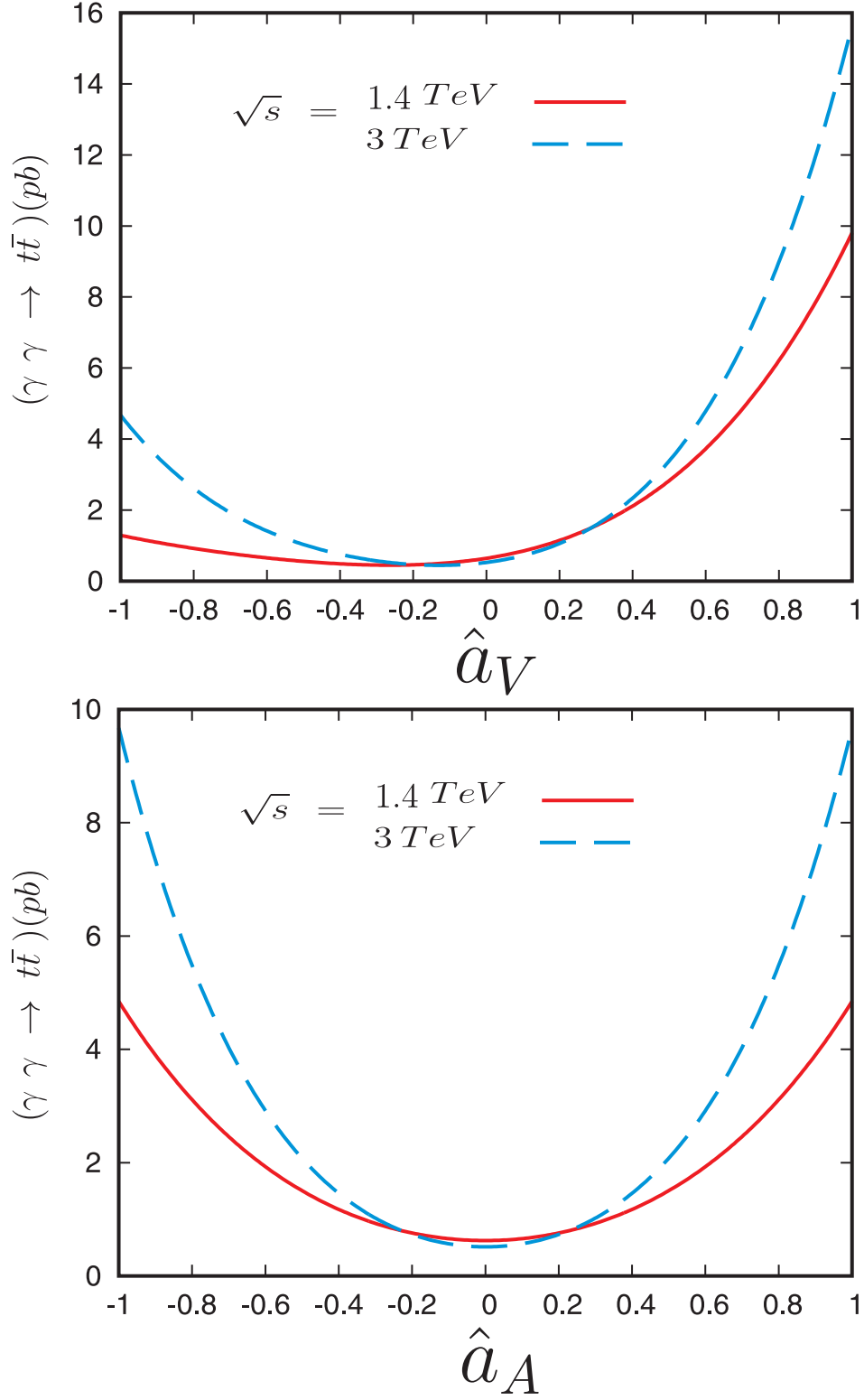


FIG. 3: The total cross sections of the process $\gamma\gamma \rightarrow t\bar{t}$ as a function of \hat{a}_V and \hat{a}_A for two different center-of-mass energies of $\sqrt{s} = 1.4, 3 TeV$, respectively.

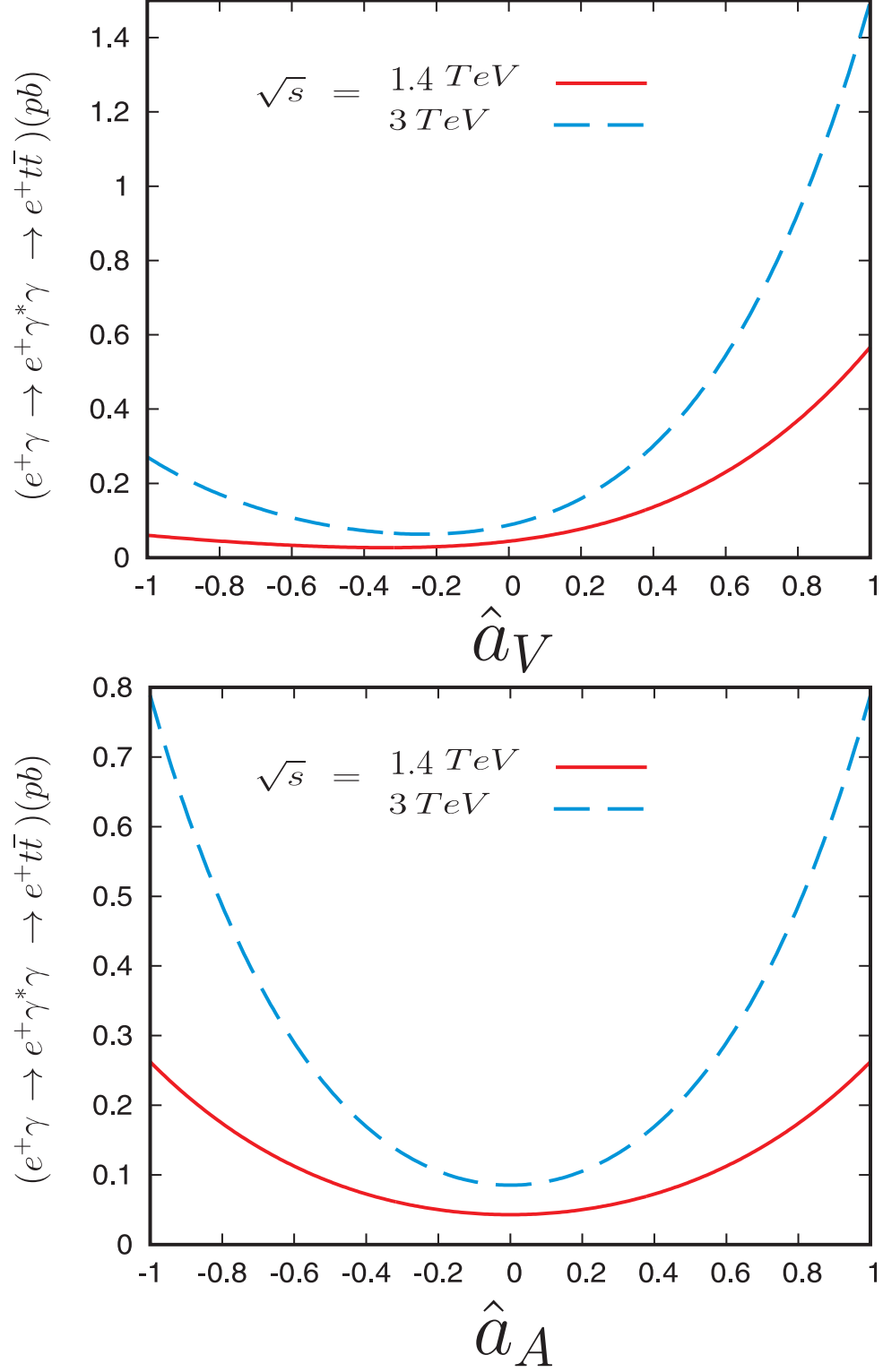


FIG. 4: Same as in Fig. 3, but for process $e^+\gamma \rightarrow e^+\gamma^*\gamma \rightarrow e^+t\bar{t}$.

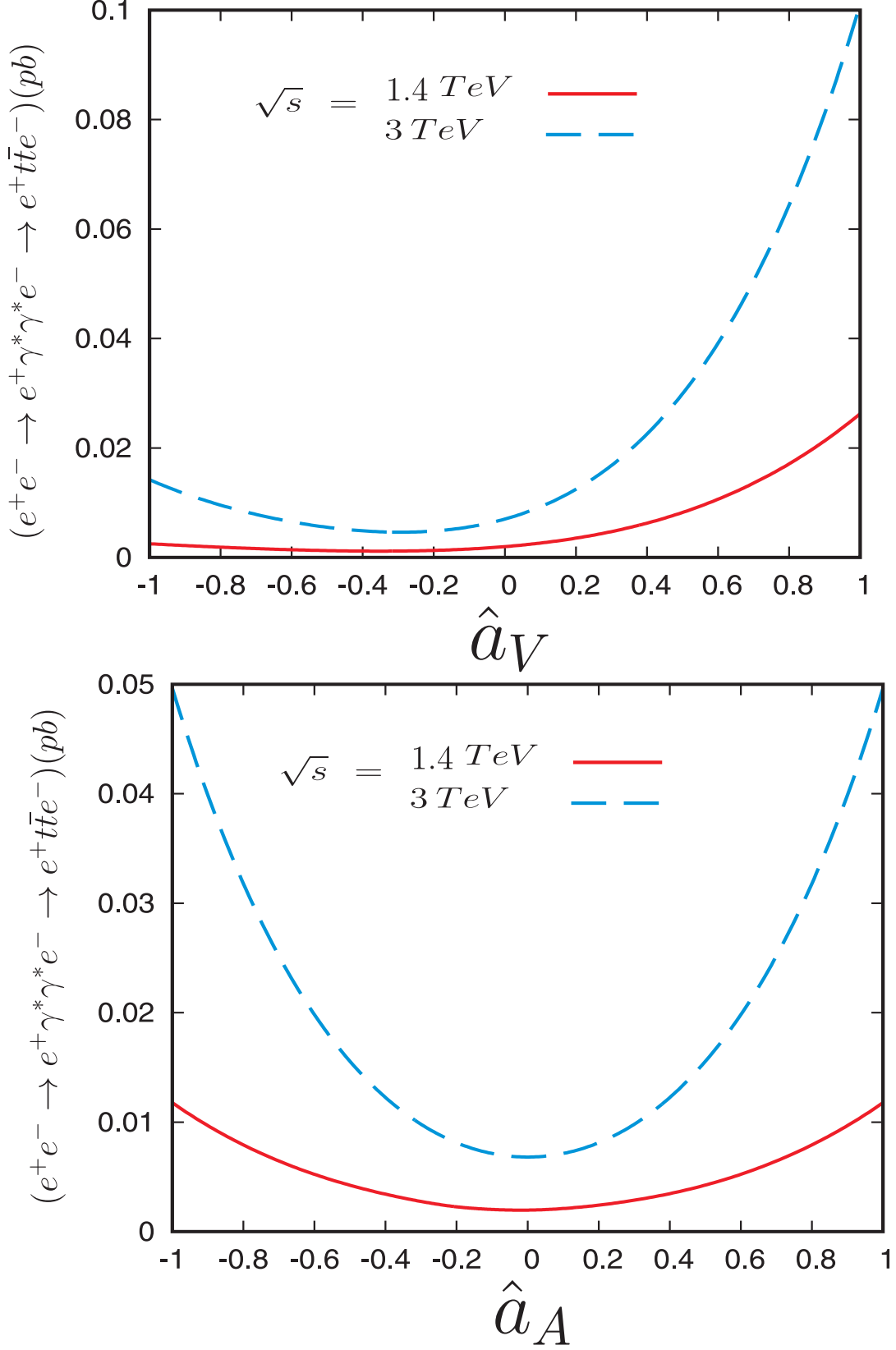


FIG. 5: Same as in Fig. 3, but for process $e^+e^- \rightarrow e^+\gamma^*\gamma^*e^- \rightarrow e^+t\bar{t}e^-$.

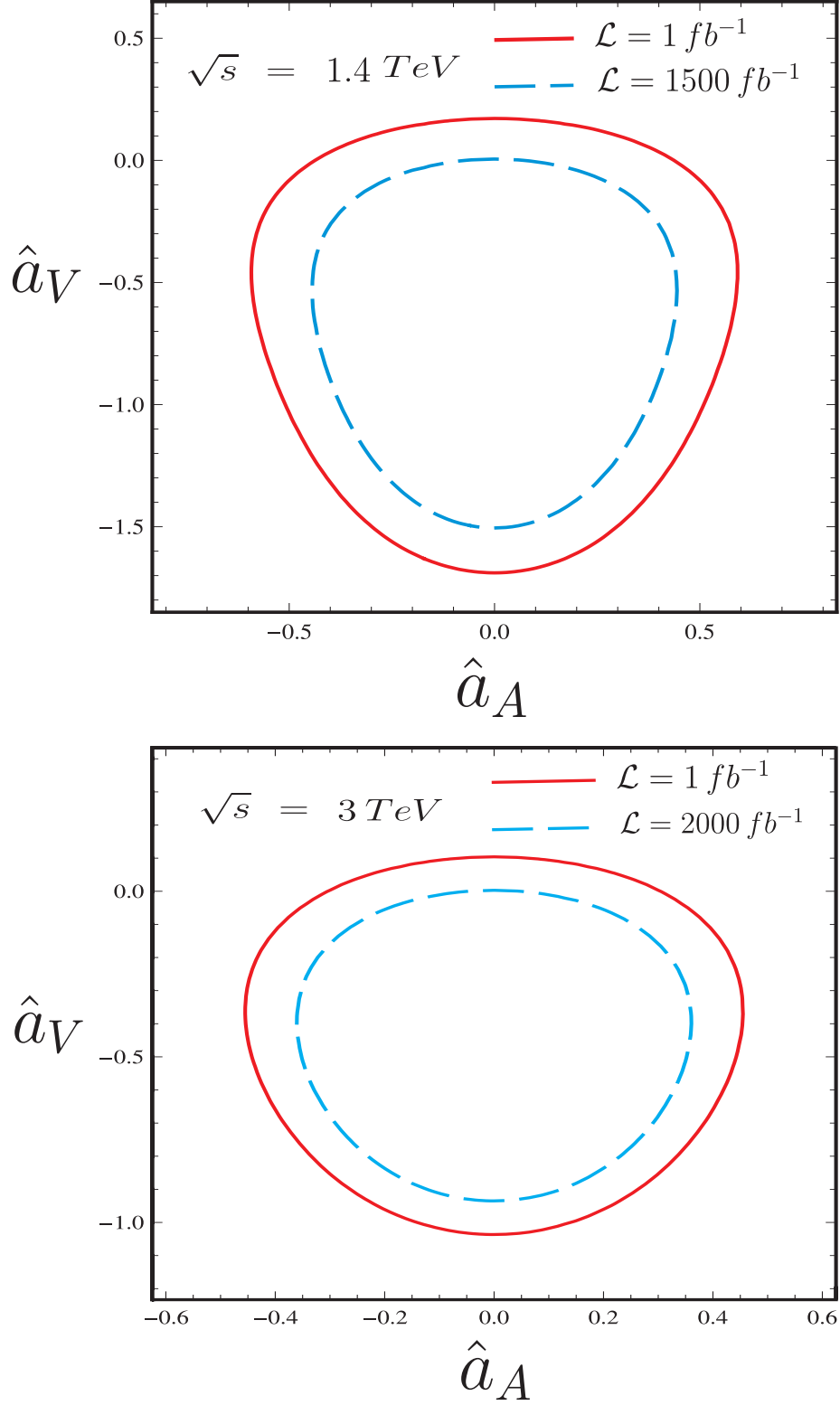


FIG. 6: Bounds contours at the 95% *C.L.* in the $\hat{a}_V - \hat{a}_A$ plane for the process $\gamma\gamma \rightarrow t\bar{t}$.

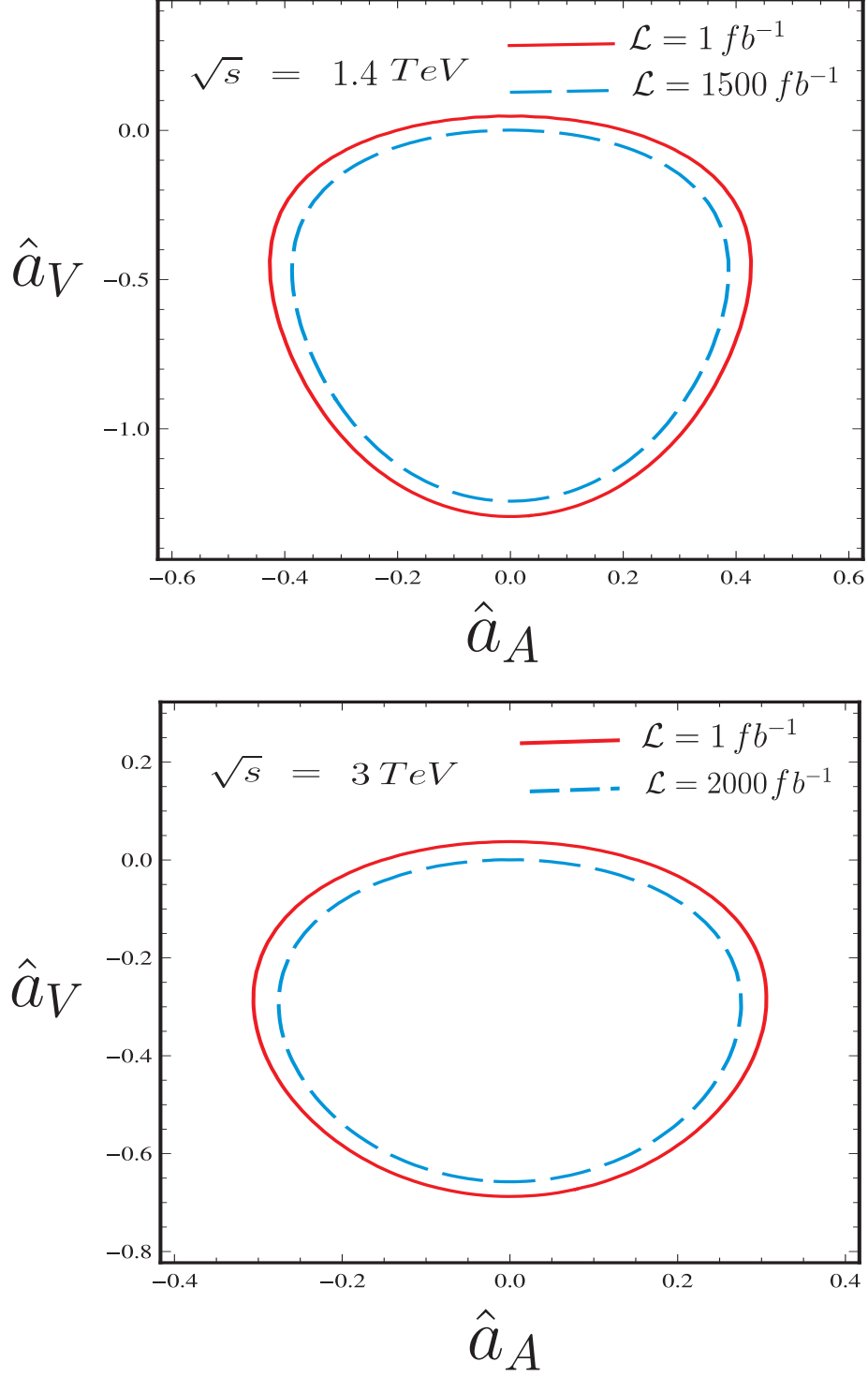


FIG. 7: Bounds contours at the 95% *C.L.* in the $\hat{a}_V - \hat{a}_A$ plane for $e^+e^- \rightarrow e^+\gamma\gamma^*e^- \rightarrow e^+t\bar{t}e^-$.

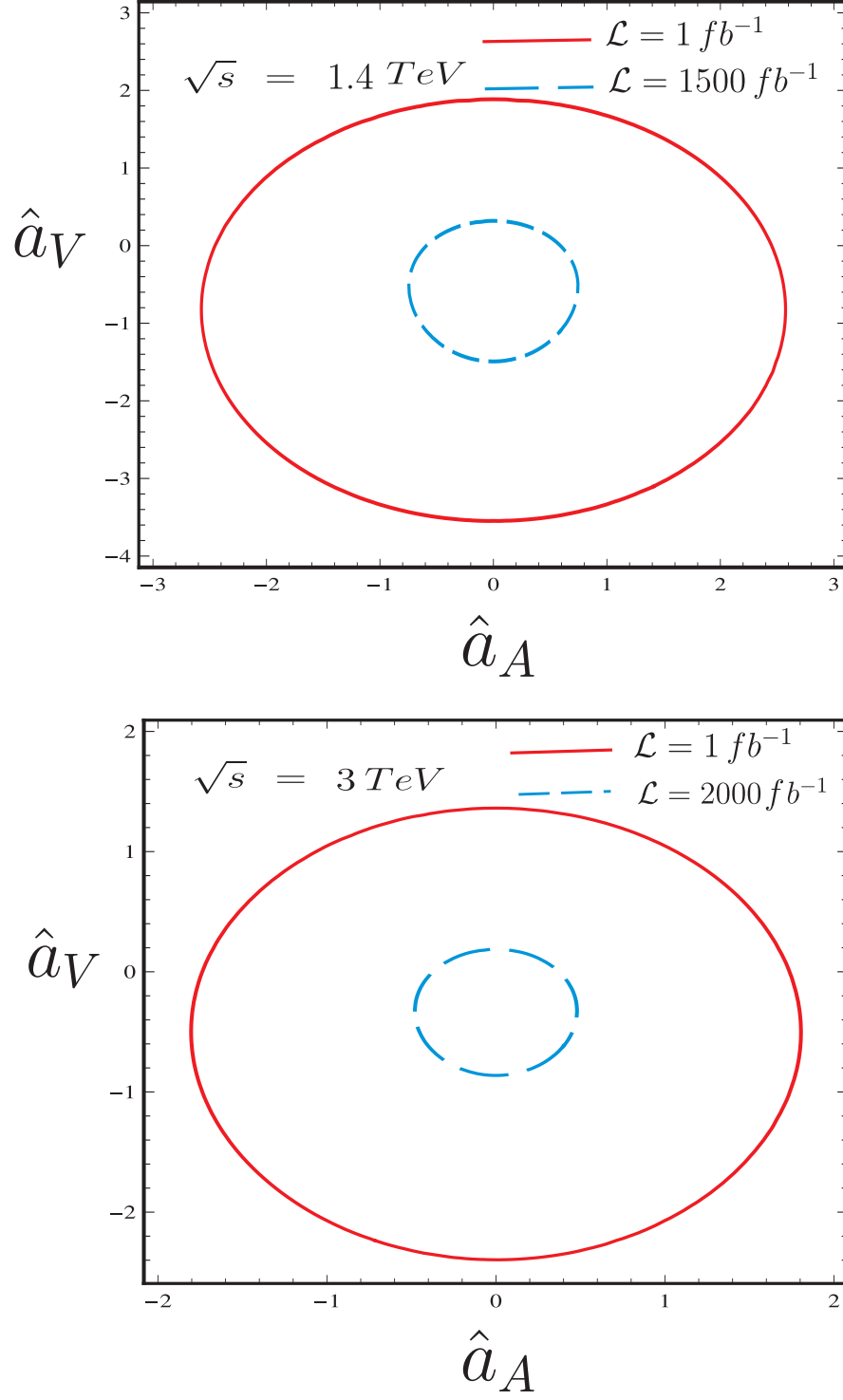


FIG. 8: Bounds contours at the 95% *C.L.* in the $\hat{a}_V - \hat{a}_A$ plane for $e^+e^- \rightarrow e^+\gamma^*\gamma^*e^- \rightarrow e^+t\bar{t}e^-$.